PRESSURE DROP THOUGH RANDOMLY PACKED BEDS OF ELLIPSOIDAL PARTICLES

Hoffmann J.E.* and Lindeque P.J.
*Author for correspondence
Department of Mechanical and Mechatronic Engineering,
Stellenbosch University,
Matieland, 7602,
South Africa,
E-mail: hoffmaj@sun.ac.za

ABSTRACT

It is postulated that packed bed of crushed rock may be approximated by mono-disperse ellipsoidal particles. Experimental testing and a CFD/DEM approach was used to determine the pressure drop across the bed for $200 \leq Re \leq 20\,000$, and for different flow directions. There was good agreement between CFD/DEM results and experimental data, but data for crushed rock is about a factor of two higher. Possible reasons are irregular shape and wide size distribution for crushed rock particles.

NOMENCLATURE

$\vec{A}$	[-]	Unit vector corresponding to long axis of particle
a,b,c	[-]	Half axes of ellipsoid
C_{ij}	[-]	Inertial resistance coefficient
$\vec{C}$	[-]	Unit vector corresponding to short axis of particle
d_p	[m]	Particle diameter
D_{ij}	[-]	Viscous resistance coefficient
ΔP	[Pa]	Pressure drop
L	[m]	Length
$\vec{R}$	[-]	Rotation vector
S_i	[Pa/m]	Momentum sink per unit volume
$\lvert\vec{U}\rvert$	[m/s]	Velocity magnitude
u_i	[m/s]	Velocity component
Vs	[m/s]	Superficial velocity
$\lvert\vec{V}\rvert$	[m/s]	Velocity magnitude
x	[m]	Cartesian axis direction
y	[m]	Cartesian axis direction
z	[m]	Cartesian axis direction
Special characters		
α	[-]	Volume fraction ratio
ε	[m]	Porosity
ϕ	[radians]	Rotation angle
μ	[Pa.s]	Fluid viscosity
ρ	[kg/m^3]	Fluid density
θ	[radians]	Angle between short axis of particle and flow direction

INTRODUCTION

The SUNSPOT cycle [1] comprise of an air standard Brayton cycle that operates during the day, and a bottoming dry-cooled Rankine cycle for night-time operation. Hot air discharged from the Brayton cycle charges the rock-bed thermal energy storage during the day. The bed is discharged at night to supply energy for steam generation to the Rankine cycle. Allen et al [2] estimated that the capital cost of rock bed storage will come in at less than half of that for an equivalent two-tank molten salt facility. Rock bed thermal energy storage is a well-established technology, especially in the building industry. Most studies were involved in predicting the transient response of the bed on a macroscopic level, and rely to some extend on local heat transfer and pressure drop correlations in the bed. Dissemination of information on a microscopic level is relatively scarce and limited to structured packings.

Heat transfer and pressure drop in packed beds have been studied for about a century. Two seminal papers stand out: Schuman [3] derived a model for transient heat transfer in an isotropic bed of particles, based upon bed-averaged parameters (particle size, packing density, particle-to-fluid contact area per unit volume, etc.), whilst Ergun [4] essentially combined the Kozeny (viscous effect) and Burke-Plummer (kinetic effect) equations into a single equation for pressure drop. Ergun used empirical data from random and structured beds of spherical and irregular particles to derive the coefficients in his equation. Although much criticized, most researchers even today benchmark their results against the Ergun equation.

Researchers realized early on that the Ergun equation does not give satisfactory results for particular applications due to its simplicity (it assumes isotropic packing, and requires only an effective particle diameter and packing density as input). Several modifications to the Ergun equation have been suggested over the years to account for particle shape and changes in packing density. In a finite bed, there is a wall affected region of about six particle diameters wide where the packing density is lower than that deeper into the bed. Consequently, Cheng and Hsu [5], Atmakidis and Kenig [6] and many others proposed an adjustment to the Ergun equation in the near-wall region. Ozahi et al [7], Singh et al [8] and Trahan et al [9] amongst others introduced modifications to the Ergun equation to account for particle shape. These modifications usually manifest in the Ergun constants becoming functions of sphericity. Langfrey et al [10] and and Sederman et al [11] in their turn suggested modifications to take packing structure into account. One would intuitively expect different pressure drops across randomly and structured packed beds, something that the Ergun equation does not predict. Others, like the German Nuclear Safety Standards Commission, or KTA for short, turned their attention to packed

beds of monodispersed spherical particles, and suggested correlations based on empirical data from a selection of packed beds of spherical particles only [12]. Others [13,14] decided to conduct their own experiments and derive correlations best suited, but also limited to their own unique applications.

A few researchers preferred a theoretical attack on the problem. Du Plessis and Woudberg [15], as well as Zang et al [16] considered flow and pressure drop through a structured bed of non-spherical, but uniformly distributed particles. Structured beds are amenable to creating representative unit cells about a single particle, and the unit cells are simply repeated to fill the entire bed. Particle shape is typically addressed via the particle drag coefficient in a free stream. Du Plessis and Woudberg concluded that the Ergun equation gave reasonable results at high packing density, but its performance is poor for low packing densities. Jiang et al [17] expanded on this idea by creating a unit cells from representative particle clusters. The same approach is followed nowadays in CFD/DEM coupling, where local porosities are exported from the DEM code to the CFD code. An example of this approach in action is given by Potgieter et al [18].

Full on CFD attacks on flow through packed beds started to appear over the last two decades. The earlier attempts were limited to small beds of spherical particles [19], whilst bed size and the number of particles increased steadily [20,21] and non-spherical particles were introduced [22]. Dumas et al [23] and Perera [24] backed their simulations up with experimental measurements. Most of these work was based on structured beds, as they are easier to generate in CFD.

CFD/DEM coupling also began to emerge, where random beds are generated in the DEM code, and the geometry is transferred to the CFD code. Louw [25] used a DEM model to create a random bed of irregular particles (six different particle shapes were created by bonding different sized spherical particles together) and modelled the flow in the interstitial volumes in CFD.

Efforts to construct the permeability tensor are mostly limited to the soil sciences [25,26].

OBJECTIVE

Crushed rock particles have a clearly discernible long and short axis, as shown in figure 1. Our hypothesis is that when poured, they tend to align with the long axis in a horizontal plane. The approached followed here is to approximate them by ellipsoidal shapes. Ellipsoids are amenable to structured and unstructured packings, making it easy to construct different packings, and extract pore level detail (void hydraulic diameter, porosity, etc.) from structured packings. At the same time, it allows one to study the effect of particle alignment.

The objective is to derive the full pressure loss tensor for flow in a packed bed, and introduce it as a momentum sink term in a computational fluid dynamics (CFD) model of a packed bed using a porous media approach.

$$S_i = -\left\{\sum_{j=1}^{3} D_{ij}\mu u_j + \sum_{j=1}^{3} C_{ij}\tfrac{1}{2}\rho\left|\vec{U}\right|u_j\right\} \quad (1)$$

Using a porous media approach would result in significant time saving when computing charging and discharging anisotropic beds, whilst retaining the directional influence of the particles on the flow through the bed.

Figure 1. Typical shapes of crushed rock

This work intends to derive the permeability tensor for flow in a rock bed using a CFD/DEM approach. It is postulated that crushed rock particles can be represented by mono-disperse volume equivalent ellipsoids with the same aspect ratio as the actual rocks.

EXPERIMENTAL WORK

Tri-axial measurements [27] of a large number of rocks were taken to obtain the mean particle aspect ratio. Particle volume was calculated from mass measurements, assuming a constant particle density of 2 650 kg/m^3 for dolerite rock [28]. These measurements resulted in ellipsoidal particles of 87.7 mm × 59.2 mm × 37.7 mm as the representative particle.

A total of 1 600 cement casts were made of the representative particles. Particles were packed in crates at 200 particles per crate. Particles were poured from the crates into a cubic expanded metal cage with side length of 652 mm. Counting the number of particles left in the last crate gave an indication of the number of particles in the crate. Void fraction was derived from the number of particles in the cage, and the particle volume. The mean void fraction for all the tests was 0.44. Between each series of tests, all the particles were removed from the cage, and a new random packing was generated for the next test series. In all, five different random packings were tested.

Stiffening bars on the faces of the cage prevents bulging. Styrofoam inserts fill the voids between the stiffening bars (see figure 2) to prevent leak flow past the sides of the cage and wind tunnels walls. The cage was then inserted into the wind tunnel (figure 3), and the test section closed up for testing in a low speed isothermal wind tunnel. Tests were done over a superficial Reynolds number range of 2 000 ≤ Re_p ≤ 20 000, using a variable speed fan. Air mass flow rate and the pressure drop across the bed were recorded. The pressure drop for an empty cage was also recorded and subtracted from the pressure drop for a packed cage.

On completion of testing through the full Reynolds number range, the cage as removed from the wind tunnel and rotated through 90° around a vertical axis, and inserted back into the tunnel for the nest series of tests. On completion of this test series, the cage was again removed from the wind tunnel, and rotated through 90° around a horizontal axis that is perpendicular to the flow direction. After the final test, the cage was removed, empties, and repacked for the next test series.

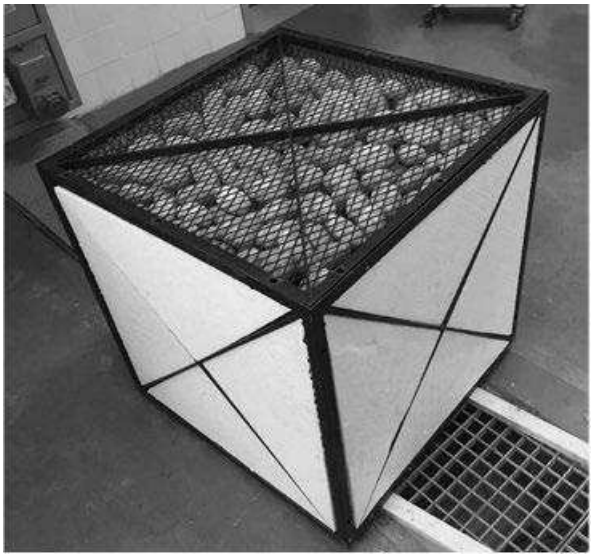

Figure 2. Expanded metal cage filled with ellipsoidal particles.

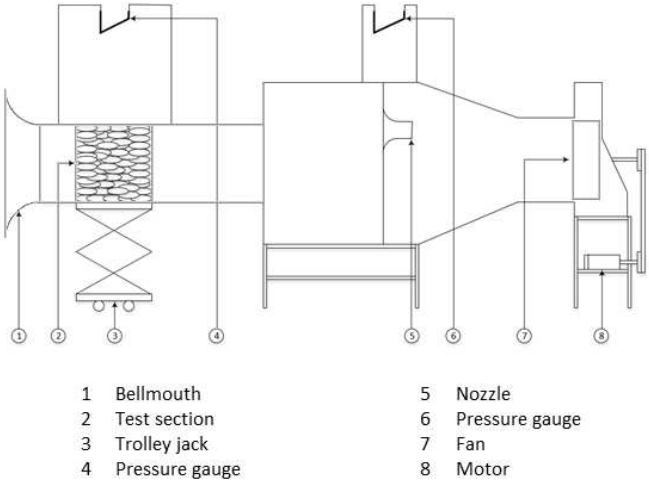

Figure 3. Schematic presentation of low speed isothermal wind tunnel.

No attempt was made to measure individual particle orientations. Such measurements could conceivably be done by hand as particles are removed one-by-one from the cage upon completion of a test series. The nature of the task and the lack of suitable instrumentation for these measurements disqualified it from the current tests.

SIMULATION

Random beds of mono-dispersed ellipsoidal particle were generated with the discrete element code (DEM) Rocky IV. Particles, with their long axes pointing in the y-direction $\{\vec{A} = (0,1,0)\}$ and short axis pointing in the z-direction $\{\vec{C} = (0,0,1)\}$, were dropped from a hopper into a 0.652 m cube box. Particle position, rotation vector $\vec{R}$ and angle of rotation ϕ around the rotation vector were extracted from the DEM results. After rotation, the orientation of the short axis was found from Rodriques's formula [29]

$$\vec{C}_{Rot} = \vec{C}\cos\phi + \left(\vec{R}\times\vec{C}\right)\sin\phi + \vec{R}\left(\vec{R}\cdot\vec{C}\right)\{1-\cos\phi\} \quad (2)$$

… and the particle's orientation with the mean flow direction is given by

$$\theta_i = \cos^{-1}\left(\frac{\vec{C}_{Rot}\cdot\vec{U}_i}{|\vec{C}_{Rot}||\vec{U}_i|}\right) \quad (3)$$

… with $\vec{U}_i$ the mean (at wind tunnel inlet) velocity vector during a test. Flow direction is taken relative to the cage orientation when packed.

Our alignment hypothesis was confirmed by orientation angles of $\theta_x = 90.01° \pm 26.92°$ and $\theta_z = 87.29° \pm 26.33°$ for horizontal flow relative to the pouring direction, and $\theta_y = -1.44° \pm 47.22°$ for vertical flow. Furthermore, the orientation angle varies in the range $-57.29° \le \theta_y \le 57.30°$. We expect the pressure drop to correlate with θ_y. However, we have insufficient data to extract this correlation coefficient.

A single ellipsoidal particle was created in the ANSYS pre-processor SpaceClaim. A Python script was written to copy the particle, rotate it along the orientation vector by and angle ϕ and translate it to its new position. A cubic box was created around the particles, and particles that fall partially outside the lid of the box were removed from the domain. The remaining particles were subtracted from the volume of the box to leave only the interstitial volumes. The close proximity of some non-touching particle faces, and small angles between touching particles did not allow prismatic cells on particle surfaces. It also gave rise to a significant number of skew cells. Hence, a tetrahedral mesh was created using proximity and curvature size functions and restricting cell size and growth. The tetrahedral meshes contain about 220 million cells (hardware constraint of 256 GB RAM 16 core Xeon machine). Mesh size was reduced by converting tetrahedral cells into about 50 million polyhedral cells.

Due to the low velocities expected in a packed bed, incompressible flow was assumed. A constant velocity boundary condition was prescribed at the domain inlet, and a pressure boundary at the outlet. Side walls of the wind tunnel and particles were modelled as smooth walls. Second order discretization schemes, with warped cell correction, were selected for all flow variables. Under-relaxation was required to get converged solutions.

Residuals dropped by about two orders of magnitude, and then become stuck. The pressure at the inlet boundary was monitored, and convergence declared if the inlet pressure remains constant for at least 200 iterations. This was usually achieved in less than 1 000 iterations.

The inlet velocity was adjusted between runs to give pressure drop data spanning a Reynolds number range of at least one order of magnitude. There was some overlap between the CFD and experimental ranges, with the CFD simulations targeting Reynolds numbers an order of magnitude lower than those in the experiments to expand the overall data range.

We were limited by the use of a demonstration licence for the Rocky DEM code, and could not pursue multiple packings to demonstrate the effect of particle alignment with flow direction adequately. Hence, we turned our attention to validation of CFD results against our experimental data.

VALIDATION

Computational results for the vertical flow direction are shown in figure 3. Agreement between CFD and experimental data is quite good. Unlike the experiments that were repeated for different packings, we could only generate one DEM pack before our Rocky license expired. Furthermore, the packing density for the DEM model was about 10 % higher than the average for the experiments. Test data with crushed rock [28] from the same batch that was used to define the representative particle is significantly higher than that for ellipsoidal particles. It is expected that particle irregularity is responsible for the large difference in bed resistance for crushed rock particles and their representative ellipsoidal particles. There is a significant difference in the pressure drop in the vertical, compared to the two horizontal directions with regards to the cage orientation upon packing, as shown in figure 4.

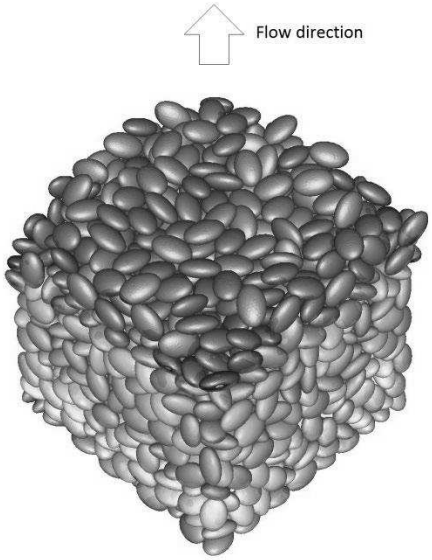

Figure 3. Pressure contours on rock surfaces for vertical upwards flow.

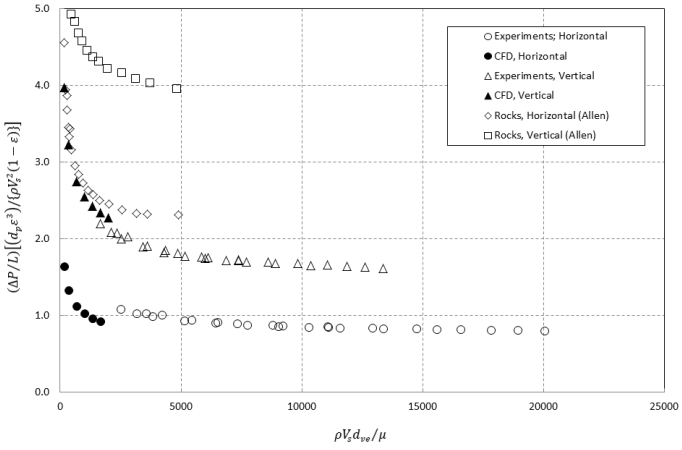

Figure 4. Experimental data for randomly packed beds.

The high resistance for vertical flow through the packed bed meant that the fan could not deliver the same flow rate for vertical flow compared to horizontal flow. At Reynolds numbers below about 2 000, the pressure drop could not be measured reliably with the available instrumentation. We could expand our Reynolds number range by using CFD/DEM data to augment the experimental data.

ROCK BED APPLICATION AND RESULTS

A linear regression on the combined experimental (higher Reynolds numbers) and simulation (lower Reynolds numbers) data shown in figure 4 yields the following coefficients for D_{ij} and C_{ij}

$$D_{ij} = \begin{bmatrix} 2060110 & 0 & 0 \\ 0 & 2326575 & 0 \\ 0 & 0 & 2149227 \end{bmatrix}$$

… and

$$C_{ij} = \begin{bmatrix} 266.92 & 0 & 0 \\ 0 & 330.22 & 0 \\ 0 & 0 & 274.55 \end{bmatrix}$$

The current experimental set-up does not allow for the determination of off-diagonal elements of the resistance tensor. By comparison, the Ergun coefficients for spherical particles of the volume equivalent diameter are $\alpha = 6.3037 \times 10^{-6}$ and $C_2 = 389.98$ respectively, where the simplified form of equation (1) for an isotropic resistance suggested by Ergun is

$$S_i = -\left\{\frac{\mu}{\alpha}u_i + \frac{1}{2}C_2\rho\left|\vec{U}\right|u_i\right\} \quad (4)$$

A hypothetical packed bed inside a thermally insulated containment structure, as shown in figure 5 was simulated. Air enters through a pipe into the plenum above the rock bed, and exits through another pipe partially embedded inside the rock bed at the bottom. The outlet pipe embedded inside the rock bed has porous walls, across which a porous jump boundary condition was prescribed. The same mesh was used for both the anisotropic resistance model, as well as the isotropic Ergun resistance model. Isothermal flow was assumed in both cases.

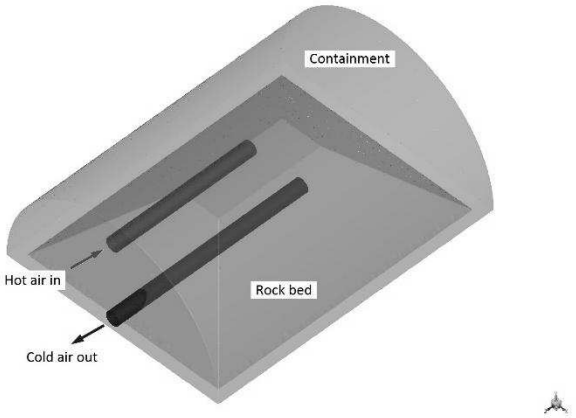

Figure 5. Computational domain for flow through rock bed.

Velocity components from the anisotropic model were exported as user defined scalars, and read into the Ergun model. Custom

field functions of the (anisotropic) velocity magnitude, and the relative difference in velocity magnitude between the two models were generated. From figure 6, it is clear that the velocity difference between the two models as a percentage, is rather large. By implication, one would expect the temperature profiles in the rock bed differ significantly as well. This would in turn affects the charging/discharging efficiency of the bed.

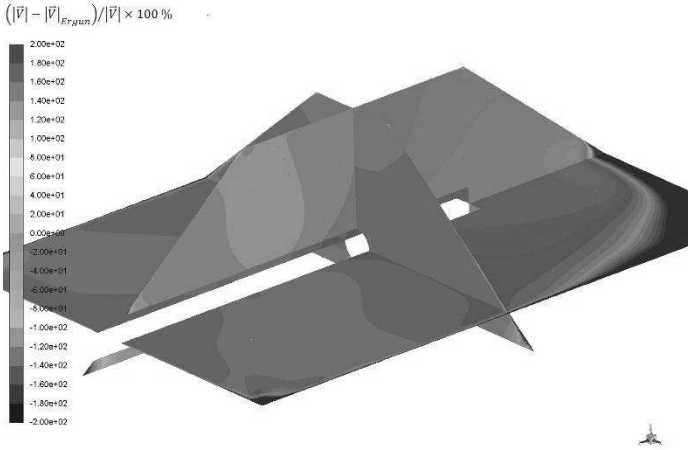

Figure 6. Relative velocity difference between Ergun- and ansiotropic resistance models.

CONCLUSION

Approximating crushed rock particles by monodisperse ellipsoids are mathematically convenient to extract particle alignment and aspect ratio data for further processing. Castings of about 1 600 ellipsoidal particles were made and the pressure drop across a packed bed was measured in an isothermal wind tunnel. The CFD/DEM approach was validated against test data, as illustrated by the good agreement between the experimental and computational data. The CFD data was used to augment experimental data in the low Reynolds number range.

Viscous and inertial resistance coefficients for an anisotropic packing of ellipsoidal particles were extracted from the experimental and CFD data. These coefficients were introduced into a packed bed simulation, using a porous media approach. Results were compared against the Ergun equation for particles with the same volume equivalent diameter. Local differences in the velocity magnitude between the two models were rather large, which may have a significant impact on the charging/discharging efficiency of a rock bed thermal energy storage system.

However, large differences in pressure drop exist between tests with ellipsoidal particles and actual packed beds of crushed rock. It is expected that irregular particle shape, and the wide distribution of particle sizes in crushed rock are responsible for it. According to Rodriguez et al [27], aspect ratio, sphericity and roundness (angularity) are required to properly describe particle shape. The latter two particle properties can be measured by 3D scanning of a large number of particles.

FURTHER WORK

Further testing is planned with a spherical cage that can be rotated in small increments in both the azimuthal and elevation angles. This would help us in correlating bed resistance with particle orientation, and to determine the off-diagonal elements of the permeability tensor to be used in porous medium approximations of the flow through rock beds. A non-thermal equilibrium model for heat transfer in a packed bed, based on combined experimental and simulation data is planned.

REFERENCES

[1] Kröger D.G., Reuter H.and Gauché P., SUNSPOT solar thermal technology package,http://www.innovus.co.za/ pages/english/technology/our-technologies-and-spin-out-companies/engineering-and-renewable-energy/sunspot.php

[2] Allen K.G. et al, Rock bed thermal storage: Concepts and costs, *AIP Conference Proceedings*, Vol. 1734, Paper 050003, 2016.

[3] Schumann T.E.W., Heat transfer: a liquid flowing through a porous prism, *Journal of the Franklin Institute*, Vol. 208, 1928, pp. 405 – 416.

[4] Ergun S., Fluid flow through packed columns, *Chemical Engineering Progress*, Vol. 48, 1952, pp. 89 – 94.

[5] Cheng P. and Hsu C.T., Fully-developed, forced convective flow through an annular packed sphere-bed with wall effects, *International Journal of Heat and Mass Transfer*, Vol. 29, 1986, pp. 1843 – 1853.

[6] Atmakidis T. and Kenig E. Y., CFD-based analysis of the wall effect on the pressure drop in packed beds with moderate tube/particle diameter ratios in the laminar flow regime, *Chemical Engineering Journal*, Vol. 155, 2009, pp. 404 – 410.

[7] Ozahi E., Gundogdu M.Y. and Caprinioglu M.O., , A modification on Ergun's correlation for use in cylindrical packed bedswith non-spherical particles, *Advanced Powder Technology*, Vol, 19, 2008, pp. 369 – 381.

[8] Singh R., Saini R.P. and Saini J.S., Nusselt number and friction factor correlations for packed bed solar energy storage system having large sized elements of different shapes, *Solar Energy*, Vol. 80, 2006, pp. 760 – 771.

[9] Trahan J. et al, Evaluation of pressure drop and particle sphericity for an air-rock bed thermal energy storage system, *Energy Procedia*, Vol. 57, 2014, pp. 633 – 642.

[10] Lanfrey P.Y., Kuzeljevic Z.V. and Dudukovic M.P., Tortuosity model for fixed beds randomly packed with identical particles, *Chemical Engineering Science*, Vol. 65, 2010, pp. 1891 – 1896.

[11] Sederman A.J. et al, Structure flow correlations in packed beds, *Chemical Engineering Science*, Vol. 53, 1998, pp. 2117 – 2128.

[12] Nuclear Safety Standards Commission KTA, (1981), Reactor Core Design of High-Temperature Gas-Cooled Reactors Part 3: Loss of Pressure through Friction in Pebble Bed Cores, http://www.kta-gs.de/e/standards/3100/3102_3_engl_1981_03.pdf.

[13] Allen K.G., van Backstöm T.W. and Kröger D.G., Packed bed pressure drop dependence on particle shape, size distribution, packing arrangement and roughness, *Powder Technology*, Vol. 246, 2013, pp. 590 – 600.

[14] Li L. and Ma W., Experimental Study on the Effective Particle Diameter of a Packed Bed with Non-Spherical Particles, *Transport in Porous Media*, Vol. 89, 2011, pp. 35 – 48.

[15] Du Plessis J.P. and Woudberg S., Pore-scale derivation of the Ergun equation to enhance its adaptability and generalization, *Chemical Engineering Science*, Vol. 63, 2008, pp. 2576 – 2586.

[16] Zang C. et al, Numerical Modeling of Three Dimensional Heat Transfer and Fluid Flow Through Interrupted Plates Using Unit Cell Scale, *Proceedings of IHTC-15*, 2014, Kyoto.
[17] Jiang Y. et al, Single phase flow modeling in packed beds: discrete cell approach revisited, *Chemical Engineering Science*, Vol. 55, 2000, pp. 1829 – 1844.
[18] Potgieter M.C., Du Toit C.G. and Kruger J.H., A 3D CFD model of the flow and heat transfer inside an unstructured bed of uniform spheres, *SACAM 2016*, Potchefstroom, 2016.
[19] Lochtenberg A.A. and Dixon A.G., Computational fluid dynamics studies of fixed bed heat transfer, *Chemical Engineering and Processing*, Vol. 37, 1998, pp. 7 – 21.
[20] Jafari A. et al, Modeling and CFD simulation of flow behavior and dispersivity through randomly packed bed reactors, *Chemical Engineering Journal*, Vol. 144, 2008, pp. 476 – 482.
[21] Guo X. and Dai R., Numerical simulation of flow and heat transfer in a random packed bed , P*articuolgy*, Vol. 8, 2010, pp. 293 – 299.
[22] Yang J. et al, Forced convective heat transfer in novel structured packed beds of particles, *HEFAT 2011*, Pointe Aux Piments, 2011.
[23] Dumas T., Lesage F. and Latifi M.A., Modelling and measurements of the velocity gradient and local flow direction at the pore scale of a packed bed, *Chemical Engineering Research and Design*, Vol. 88, 2010, pp. 379 – 384.
[24] Perera D., Heat transfer and flow in packed beds with nuclear magnetic resonance microscopy and computational fluid dynamics, M. Eng. Thesis, Montana State University, 2017.
[24] Louw A.D.R., Discrete and porous computational fluid dynamics modelling of an air-rock bed thermal energy storage, M. Eng. Thesis, Stellenbosch University, 2014.
[25] Renard P., Laboratory determination of the full permeability tensor, Journal of Geophysical Research, Vol. 106, 2001, pp. 26443 – 26452.
[26] Lang P.S., Paluszny A., and Zimmerman R.W., Permeability tensor of three-dimensional fractured porous rock and a comparison to trace map predictions, Journal of Geophysical Research: Solid Earth, Vol. 199, 2014, pp. 6288 – 6307.
[27] Rodriguez J.M., Ediskär T. and Knutsson S., Particle shape quantities and measurement techniques – a review, The Electronic Journal of Geotechnical Engineering, Vol. 18, 2013, pp. 169 – 198.
[28] Allen K.G., Rock bed thermal storage for concentrating solar power plants, PhD Thesis, Stellenbosch University, 2014.
[29] Spiegel M.R., Mathematical handbook of formulas and tables, McGraw-Hill Inc., 1968.